

ORIGINAL ARTICLE

# Synthesis and optical and photovoltaic properties of dithienosilole–dithienylpyridine and dithienosilole–pyridine alternate polymers and polymer– $B(C_6F_5)_3$ complexes

Daiki Tanaka<sup>1</sup>, Joji Ohshita<sup>1</sup>, Yousuke Ooyama<sup>1</sup> and Yasushi Morihara<sup>2</sup>

Donor–acceptor (D–A)-type alternate polymers were synthesized, with either dithienylidithienosilole or dithienosilole as the donor and pyridine as the acceptor, and they exhibited broad absorption peaks at approximately 520 nm. Complex formation of the polymers with  $B(C_6F_5)_3$  was examined, revealing even broader absorption peaks, with the edges red-shifted relative to the parent polymers. Blend films of the polymers and their complexes with PC<sub>71</sub>BM were applied as active layers in bulk heterojunction-type polymer solar cells, resulting in a power-conversion efficiency (PCE) of 0.25–1.33%. Treatment of TiO<sub>2</sub> electrodes with the polymer solutions led to the attachment of polymer on the TiO<sub>2</sub> surface. Using the resulting polymer-attached TiO<sub>2</sub> electrodes, dye-sensitized solar cells were fabricated with a PCE of 0.54–0.55%.

*Polymer Journal* (2013) 45, 1153–1158; doi:10.1038/pj.2013.46; published online 8 May 2013

**Keywords:** boron–pyridine complex; donor–acceptor interaction; photovoltaic polymer

## INTRODUCTION

Solar cells based on organic materials (organic photovoltaic cells (OPVs)), including bulk heterojunction (BHJ)-type polymer solar cells (PSCs) and dye-sensitized solar cells (DSSCs), receive a great deal of attention because of their advantages, such as their low production cost, potential flexibility and tunable cell color, over conventional inorganic cells. Donor–acceptor (D–A)-type compounds and polymers have been studied extensively as key materials for OPVs.<sup>1–3</sup> Their broad, red-shifted absorptions arising from a low bandgap make it possible to utilize the wide range of sunlight wavelengths, and their polar structures facilitate photo-induced charge separation in this system.

Silicon-bridged bithiophene, particularly dithienosilole (DTS), has been often employed as a building unit for  $\pi$ -conjugated functional materials.<sup>4–8</sup> DTS exhibits enhanced conjugation due to the orbital interaction between the silicon  $\sigma$ -bonds and the bithiophene  $\pi$ -system, as well as a highly planar tricyclic structure.<sup>9</sup> Recently, several D–A-type compounds and polymers containing DTS units as the donor were prepared; they were shown to interact efficiently with acceptor groups, such as benzothiadiazole,<sup>10</sup> thiazolothiazole<sup>11–13</sup> and thienopyrrolodione,<sup>14</sup> and their applications to high-performance BHJ-type PSCs were explored.

Recently, Bazan and coworkers found that a DTS–benzothiadiazole oligomer formed a complex with  $B(C_6F_5)_3$  through N–B coordination

to enhance the D–A interaction in the backbone, which shifted the absorption band significantly to a lower-energy region (Scheme 1).<sup>15</sup> Similar studies concerning complex formation with dithienocyclopentadiene–benzothiadiazole and dithienocyclopentadiene–pyridinethiadiazole oligomers and polymers have also been conducted.<sup>16</sup> Hayashi *et al.*<sup>17,18</sup> demonstrated formation of similar complex polymers as insoluble solid films from two routes, treatment of fluorene– and bithiophene–pyridine polymer films with  $BF_3\text{--}OEt_2$  and oxidative electro-polymerization of a dithienylpyridine– $BF_3$  complex.

However, there have been no reports concerning the photovoltaic applications of such N–B complex polymers, despite the fact that complex formation can enhance the D–A interaction and result in broad, red-shifted absorption peaks. To explore these photovoltaic applications, we prepared new soluble DTS–pyridine alternate polymers, with the hypothesis that the high Lewis basicity of pyridine would induce a strong interaction between the polymers and  $B(C_6F_5)_3$  molecules, thereby permitting us to study applications of these complex polymers to BHJ-type PSCs. We also examined the attachment of polymer to the TiO<sub>2</sub> surface due to the coordinative interaction between the polymer pyridine units and the Lewis acid sites of TiO<sub>2</sub>, and we subsequently used the resulting polymer-attached TiO<sub>2</sub> material in DSSCs.

<sup>1</sup>Department of Applied Chemistry, Graduate School of Engineering, Hiroshima University, Higashi-Hiroshima, Japan and <sup>2</sup>Synthesis Research Laboratory, Kurashiki Research Center, Kuraray Co. Ltd., Kurashiki, Japan  
Correspondence: Professor J Ohshita, Department of Applied Chemistry, Graduate School of Engineering, Hiroshima University, Higashi-Hiroshima 739-8527, Japan.  
E-mail: jo@hiroshima-u.ac.jp

Received 31 January 2013; revised 6 March 2013; accepted 12 March 2013; published online 8 May 2013

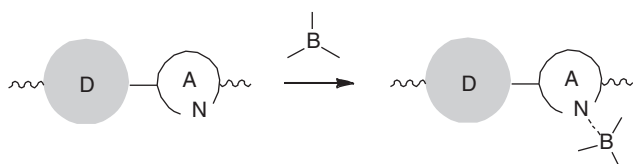
## EXPERIMENTAL PROCEDURE

## General

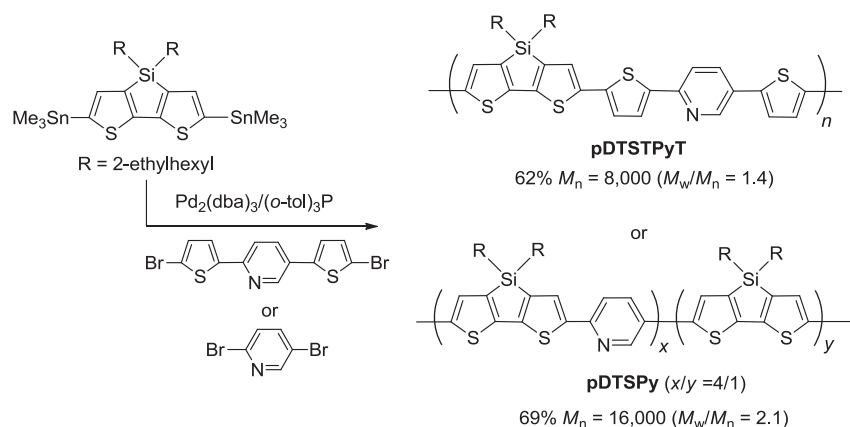
All reactions were carried out under dry argon. Chlorobenzene, which was used as the reaction solvent, was distilled from  $\text{CaH}_2$  and stored over activated molecular sieves until use. The monomers, 2,6-bis(trimethylstannyl)-4,4-bis(2-ethylhexyl)dithienosilole<sup>10</sup> and 2,5-bis(5-bromo-2-thienyl)pyridine,<sup>19</sup> were prepared as reported in the literature. Nuclear magnetic resonance (NMR) spectra were recorded on a Varian System-500 spectrometer (Agilent Inc., Santa Clara, CA, USA). Ultraviolet (UV) absorption spectra were measured on a HITACHI U2910 spectrophotometer (Hitachi High-Tech Co., Tokyo, Japan). Gel permeation chromatography (GPC) was carried out at ambient temperature using serially connected Shodex KF2001 and KF2002 columns with tetrahydrofuran as the eluent.

## Synthesis of DTS-pyridine alternate polymers

A mixture of 2,6-bis(trimethylstannyl)-4,4-bis(2-ethylhexyl)dithienosilole (0.39 g, 0.52 mmol), 2,5-bis(5-bromo-2-thienyl)pyridine (0.21 g, 0.52 mmol),  $\text{Pd}_2(\text{dba})_3$  (10 mg, 0.010 mmol), (*o*-tolyl)<sub>3</sub>P (25 mg, 0.083 mmol) and chlorobenzene (30 ml) was placed in a 50-ml two-necked flask fitted with a reflux condenser, and the mixture was heated under reflux for 5 days (Scheme 2). The resulting mixture was allowed to cool to room temperature, and a 30-ml aqueous solution of sodium *N,N*-diethyldithiocarbamate trihydrate (3.1 g) was added; the mixture was then heated to 80 °C for 2 h. The organic layer was separated and washed in the following order: first water, followed by 3 vol% acetic acid aqueous solution, and finally water again. The organic layer was dried over anhydrous magnesium sulfate, and the solvent was removed under vacuum. Reprecipitation of the residue from chloroform/methanol gave polymeric substances, which were then placed in a Soxhlet apparatus and washed with, in the following order: hot methanol, ethanol and hexane. Finally, the residue, which had remained insoluble in those hot solvents, was extracted using hot chloroform. The chloroform solution was then poured into hexane,



Scheme 1 Complex formation of D-A-type polymers with borane.



Scheme 2 Synthesis of DTS-pyridine polymers with yields and molecular weights following reprecipitation. Molecular weights were determined by GPC, relative to polystyrene standards.

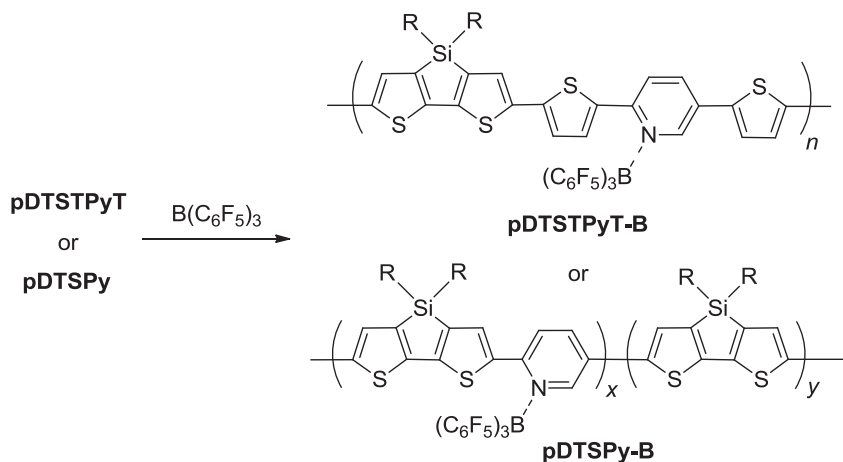
and the precipitates were collected to provide **pDTSTPyT** (0.21 g, 62%) as red-purple solids: m.p. > 300 °C;  $M_n = 11,000$ ,  $M_w/M_n = 2.1$ ; <sup>1</sup>H NMR ( $\delta$  in  $\text{CDCl}_3$ , 500 MHz) 0.79–1.48 (br m, 34H, 2-ethylhexyl), 6.79–7.83 (br m, 8H, aromatic ring proton), 8.83 (br s, 1H, pyridylene proton on C6); <sup>13</sup>C NMR ( $\delta$  in  $\text{CDCl}_3$ , 125 MHz) 10.83, 14.29, 17.55, 23.01, 28.85, 35.16, 35.82.  $\text{Sp}^2$  carbons could not be observed, likely due to signal broadening.

Polymer **pDTSPy** was synthesized as dark red solids using the Stille coupling reaction following a procedure similar to that described above for **pDTSTPyT**. Data for **pDTSPy**: 69% yield; m.p. > 300 °C;  $M_n = 16,000$ ,  $M_w/M_n = 2.1$ ; <sup>1</sup>H NMR ( $\delta$  in  $\text{CDCl}_3$ , 500 MHz) 0.83–1.51 (br m, 34H, 2-ethylhexyl), 7.14 (br s, 0.4H, homo-coupled DTS proton), 7.37 (br s, 0.8H, DTS proton), 7.59 (br s, 0.8H, DTS proton), 7.64 (br s, 0.8H, pyridylene proton), 7.84 (br s, 0.8H, pyridylene proton), 8.00 (br s, 0.1H, terminal Br-pyridyl proton), 8.45 (br s, 0.1H, terminal Br-pyridyl proton), 8.84 (br s, 0.8H, pyridylene proton on C6), 8.97 (br s, 0.1H, terminal Br-pyridyl proton on C6); <sup>13</sup>C NMR ( $\delta$  in  $\text{CDCl}_3$ , 125 MHz) 10.84, 14.18, 17.61, 17.65, 23.02, 28.89, 35.63, 35.65, 35.92.  $\text{Sp}^2$  carbons could not be observed, likely due to signal broadening.

## Preparation of polymer-borane complex

To a solution of 43 mg of **pDTSTPyT** in 25 ml of chlorobenzene, a solution of 34 mg (1.0 equiv for pyridine unit) of tris(pentafluorophenyl)borane in 4 ml of chlorobenzene was added at room temperature (Scheme 3). The mixture was stirred for 1 day at room temperature, and the solvent was removed under vacuum to give **pDTSTPyT-B** as blue-purple solids: m.p. > 300 °C; <sup>1</sup>H NMR ( $\delta$  in  $\text{CDCl}_3$ , 500 MHz) 0.79–1.48 (br m, 34H, 2-ethylhexyl), 6.67–7.20 (br m, 3H, aromatic ring proton), 7.33–8.02 (br m, 5H, aromatic ring proton), 8.28–8.51 (br m, 1H, aromatic ring proton); <sup>11</sup>B NMR ( $\delta$  in  $\text{C}_6\text{D}_6$ , 160 MHz) –4.06.

Polymer-borane complex **pDTSPy-B** was prepared by treating **pDTSPy** with tris(pentafluorophenyl)borane (0.63 equiv for pyridine unit) and appeared as a purple solid, following a procedure similar to that described above for **pDTSTPyT-B**. In this experiment, a polymer containing non-coordinated pyridine units was obtained. Data for **pDTSPy-B**: m.p. > 300 °C; <sup>1</sup>H NMR ( $\delta$  in  $\text{CDCl}_3$ , 500 MHz) 0.71–1.56 (br m, 34H, 2-ethylhexyl), 7.42–7.52 (br m, 0.8H, DTS proton), 7.58–7.69 (br m, 0.4H, aromatic ring proton), 7.78–7.93 (br m, 0.8H, aromatic ring proton), 8.05–8.12 (br m, 0.8H, aromatic ring proton), 8.17–8.25 (br m, 0.8H, aromatic ring proton),



**Scheme 3** Formation of the complex polymers.

8.33–8.50 (br m, 0.8H, aromatic ring proton), 8.87 (br s, 0.18H, boron-free pyridylene proton on C6), 8.95 (br s, 0.02H, boron-free terminal Br–pyridyl proton on C6); the integrations could not be determined exactly due to signal broadening, and thus, approximate values are provided here;  $^{11}B$  NMR ( $\delta$  in  $C_6D_6$ , 160 MHz) –4.00.

#### Fabrication of PSCs

Tin-doped indium oxide (ITO)-coated glass substrates were cleaned using a routine cleaning procedure, which included sonication in, in this order, detergent, distilled water, acetone and 2-propanol.<sup>20</sup> The ITO surface was cleaned further by exposure to ozone for 10 min, and a layer of PEDOT:PSS (poly(2,3-dihydrothieno-1,4-dioxin)-poly(styrenesulfonate)) with a thickness of 30 nm was spin-coated onto the cleaned ITO substrate immediately thereafter. The PEDOT:PSS-coated ITO substrate was heated at 150 °C for 10 min, onto which a solution of the polymer:PC<sub>71</sub>BM blend in *o*-dichlorobenzene containing diiodooctane (2.5 vol%) was spin-coated after filtering through a 0.45- $\mu$ m polytetrafluoroethylene syringe filter. Device fabrication was completed by depositing a LiF (0.5 nm) and Al (80 nm) cathode as the top electrode onto the polymer layer at  $10^{-6}$  torr. After annealing of the PEDOT:PSS, all the handling was performed in a glove box equipped with a vacuum-deposition apparatus, and the devices were evaluated in an inert atmosphere as follows.

The current density–voltage ( $J$ – $V$ ) characteristics of the PSCs were investigated under illumination with a 100 mW cm<sup>-2</sup> (AM 1.5 G) simulated solar light from a Peccell PEC-L11 solar simulator (Peccell Technologies, Inc., Kanagawa, Japan). The data were recorded with a Keithley 2400 source-measure unit (Keithley Instruments Inc., Cleveland, OH, USA). The incident photon-to-current conversion efficiency (IPCE) was measured as a function of wavelength from 300–900 nm with a halogen lamp as the light source, and calibration was performed with a silicon reference photodiode. The thickness of the thin film was measured with a Veeco Dektak 8 surface profilometer, with an accuracy of  $\pm 5$  nm.

#### Fabrication of DSSC

Into a ball-milling apparatus, 1.3 g of TiO<sub>2</sub> (Degussa P-25, 80% anatase + 20% rutile) in air was placed. Deionized water (1.86 ml) was added to this powder in six portions, and the mixture was ground and mixed at ambient temperature at 300 r.p.m. for 10 min after each addition. Then, the mixture was further mixed with 80 mg of PEG and 3–5 drops of nitric acid by ball-mill rolling at 300 r.p.m. for 2–3 h

to give a TiO<sub>2</sub> slurry. A TiO<sub>2</sub> (5 × 5 mm<sup>2</sup>) layer was prepared by casting the slurry on a fluorine-doped tin oxide (FTO) glass plate, which was then baked in air at 500 °C for 30 min. The TiO<sub>2</sub>-coated FTO glass plate was immersed in a chloroform solution of a polymer (2 g l<sup>-1</sup>) under an argon atmosphere for 1 day at room temperature. The plate was washed thoroughly with chloroform and was air-dried at room temperature. Finally, a DSSC was fabricated using a thin liquid layer of an acetonitrile solution containing LiI (0.5 M)/I<sub>2</sub> (0.05 M), which was sandwiched between the polymer-attached TiO<sub>2</sub>/FTO and Pt electrodes. The prepared DSSC was irradiated with a monochromatic light from the FTO side, and the photocurrent was monitored as a function of wavelength by a digital electrometer (Advantest TR-8652, Advantest Co., Tokyo, Japan).

## RESULTS AND DISCUSSION

#### Polymer synthesis

Two D–A-type polymers with alternate dithienyldithienosilole-pyridine and DTS–pyridine units (**pDTSTPyT** and **pDTSPy**) were prepared via Stille coupling reactions, as shown in Scheme 2, and were subsequently purified by reprecipitation, followed by Soxhlet extraction, as red–purple and dark red solids. These purified polymers were soluble in chloroform, tetrahydrofuran and toluene but insoluble in hexane, methanol and ethanol. The  $^1H$  NMR spectra of the polymers revealed broad peaks. The integration ratio of the  $^1H$  signals of **pDTSTPyT** was consistent with the regular structure shown in Scheme 2; however, **pDTSPy** possessed smaller integration ratios for the pyridine proton signals at 7.64, 7.84 and 8.84 p.p.m. than the theoretical ratios for the regularly arranged alternate DTS–pyridine structure, suggesting that homo-coupling of DTS units had occurred to some extent during polymerization. Similarly, competition between the homo-coupling of distannyl compounds and Stille cross-coupling has been previously reported.<sup>21</sup> The incorporation ratio of the homo-coupled units (DTS–DTS) was determined to be approximately  $x/y = 4/1$  (Scheme 2). The  $^1H$  NMR spectrum of **pDTSPy** also possessed small signals at 8.00, 8.45 and 8.97 p.p.m., which were assigned to the terminal bromopyridyl groups. The molecular weight was determined to be 10 kDa based on the NMR integration of the terminal pyridine protons, which is comparable with the  $M_n$  determined by GPC relative to polystyrene standards. One might consider the possibility of preparing polymers using reverse-type coupling reactions of bis(stannyl)pyridine and dibromodithienosilole. However, it has already been reported that a similar reaction of mono(stannyl)pyridine with dibromodithienosilole provided the

expected 2:1 coupling product, but only in low yield (12%).<sup>6</sup> Polymeric **pDTSPy** exhibited a monomodal GPC profile, whereas a bimodal distribution with peaks at  $M_n = 10\,000$  and  $63\,000$  with an area ratio of ca. 10:1 was observed for **pDTSTPyT**; however, the reason for the bimodal profile is still unclear.

### Optical properties

The prepared polymers possessed UV-Vis absorption maxima at approximately 520 nm in benzene, as shown in Figure 1 and Table 1. The absorption maxima were blue-shifted from those reported for DTS homopolymers (**pDTS**,  $\lambda_{\max} = 533\text{--}561$  nm),<sup>22,23</sup> DTS-bithiophene alternate polymers (**pDTS2T**, 544–558 nm)<sup>22,23</sup> and a DTS-pyridinothiadiazole alternate polymer (**pDTSPTA**, 732 nm)<sup>20</sup> (Scheme 4). The introduction of pyridine units into **pDTS2T** and **pDTS** appeared to hinder the planarity of the resulting  $\pi$ -conjugated systems due to steric repulsion between the C–H bonds of the adjacent thiophene and pyridine rings. It is also likely that pyridine is less electron deficient than pyridinothiadiazole, and thus,

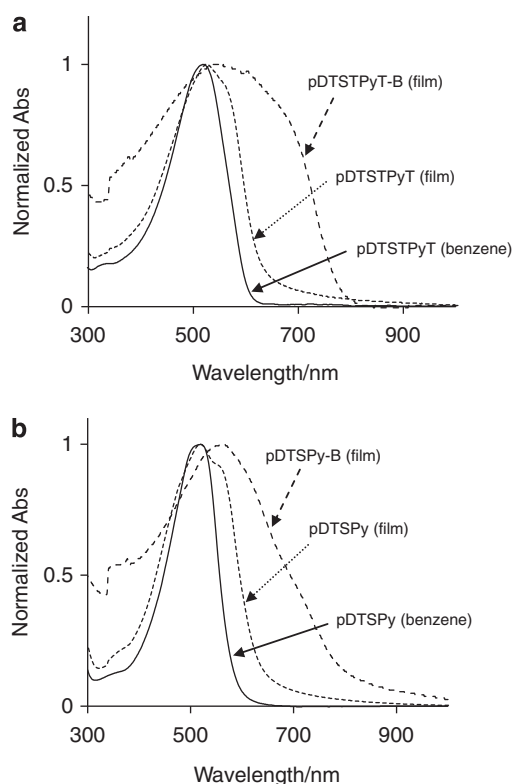


**Figure 1** UV-Vis absorption spectra of **pDTSTPyT** (a) and **pDTSPy** (b).

**Table 1** Preparation and properties of DTS-pyridine-based polymers

Polymer	UV-Vis ( $\lambda_{\max}$ nm <sup>-1</sup> )	
	In benzene	As spin-coated film
<b>pDTSTPyT</b>	519	524, 564 (sh) <sup>a</sup>
<b>pDTSPy</b>	520	519, 558 (sh) <sup>a</sup>
<b>pDTSTPyT-B</b>	534, 666 (sh) <sup>a</sup>	546, 672 (sh) <sup>a</sup>
<b>pDTSPy-B</b>	564	559

Abbreviations: DTS, dithienosilole; UV, ultraviolet.

<sup>a</sup>Shoulder.

it exhibited weaker D–A interactions with the dithienyl–DTS and DTS units in the polymers studied here.

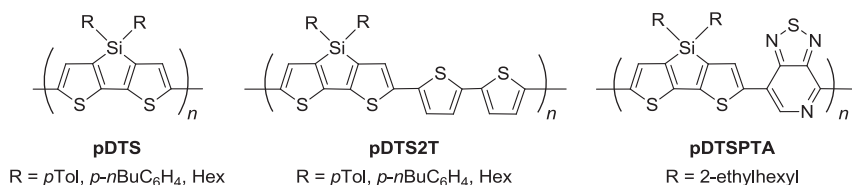
For the spin-coated films of **pDTSTPyT** and **pDTSPy**, shoulder peaks appeared at approximately 560 nm, as seen in Figure 1. This result is most likely due to stacking of the  $\pi$ -conjugated polymer chains, which indicates that there is an interchain interaction in the films, although the absorption maxima were affected slightly by the polymer state (that is, solution or film). Strong interchain interactions are important factors for BHJ-type PSC materials, because they accelerate carrier transport in the films.

### Complex formation with $B(C_6F_5)_3$

Complex formation between the polymers and  $B(C_6F_5)_3$  was monitored by UV-Vis absorption spectrophotometry, as shown in Figure 2. As  $B(C_6F_5)_3$  was added to the solutions of **pDTSTPyT** and **pDTSPy** in benzene, the solution changed color from red to purple. Simultaneously, the absorbance of the UV-Vis bands of the parent polymers decreased, and new bands appeared at longer wavelengths, which became more intense with increasing concentration of  $B(C_6F_5)_3$ . This result is in good agreement with the previously reported<sup>15–18</sup> optical properties of similar complexes of pyridine-containing polymers with borane, and it clearly indicates that complex formation reduces the polymer band gap, thereby potentially allowing for fine tuning of the electronic states. However, the changes were not completely saturated when one equivalent of  $B(C_6F_5)_3$  was added, thus indicating that the coordinated and non-coordinated units were in equilibrium.

To obtain more information about complex formation, **pDTSTPyT** was treated with  $B(C_6F_5)_3$  (1.0 equiv for pyridine unit) on a preparative scale in chlorobenzene at room temperature. A similar experiment was also carried out for **pDTSPy** with a smaller ratio of  $B(C_6F_5)_3$  (0.63 equiv), because **pDTSPy** had a more sensitive response than **pDTSTPyT** to  $B(C_6F_5)_3$ . At this loading ratio, **pDTSPy** was expected to exhibit a similar UV spectral profile to **pDTSTPyT**: $B(C_6F_5)_3 = 1:1$  (Figure 2). After the solvent had evaporated from the mixtures, the residues were analyzed by NMR and IR spectroscopies and were identified as being complex polymers **pDTSTPyT-B** and **pDTSPy-B** (Scheme 3). In the <sup>1</sup>H NMR spectra, the pyridine proton signals disappeared and decreased at 8.83 and 8.84 p.p.m. for the **pDTSTPyT** and **pDTSPy** polymers, respectively. However, new broad signals attributable to the  $\alpha$ -protons of the pyridine-boron complexes of **pDTSTPyT-B** and **pDTSPy-B** appeared at 8.28–8.51 and 8.33–8.50 p.p.m., respectively. For **pDTSPy-B**, signals ascribed to complex-free units were also observed in the <sup>1</sup>H NMR spectrum. However, the signals were too broad to determine the exact incorporation ratio of the complex units. The <sup>11</sup>B NMR spectra revealed signals at –4.06 and –4.00 p.p.m. for **pDTSTPyT-B** and **pDTSPy-B**, respectively, which were high-field-shifted relative to the complex-free  $B(C_6F_5)_3$  signal. IR analysis also supports complex formation due to the characteristic N–B vibration signals at 1083 and 1085 cm<sup>-1</sup> for **pDTSTPyT-B** and **pDTSPy-B**, respectively.<sup>24</sup> We also examined titration experiments of a 2,2':5',2''-terthiophene solution in benzene upon addition of  $B(C_6F_5)_3$  via the UV-Vis absorption. However, no obvious spectral changes were found, thus indicating that the DTS units of the polymers in this study are not coordination sites.

Upon spin-coating, the complex polymers **pDTSTPyT-B** and **pDTSPy-B** readily formed thin solid films for which the UV-Vis absorption spectra are presented in Figure 1. Although the absorption maxima were not significantly shifted from those of the corresponding complex-free parent polymers, the spectra exhibited broad



Scheme 4 DTS-containing conjugated polymers (refs 21–23).

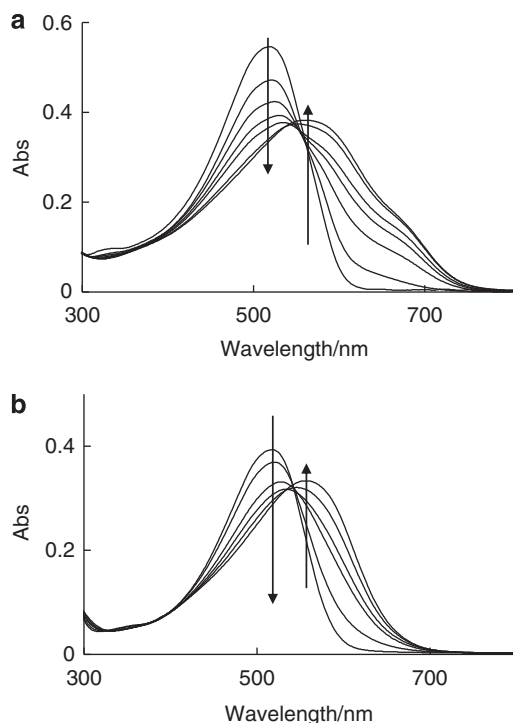


**Figure 2** UV-Vis absorption spectra of polymers at (polymer) =  $8 \times 10^{-3} \text{ g l}^{-1}$  in benzene for **pDTSTPyT** with  $(\text{B}(\text{C}_6\text{F}_5)_3)/(\text{pyridine}) = 0, 0.25, 0.5, 0.75, 1.0, 2.0, 3.0$  (a) and **pDTSPy** with  $(\text{B}(\text{C}_6\text{F}_5)_3)/(\text{pyridine}) = 0, 0.15, 0.30, 0.45, 1.2, 1.8$  (b).

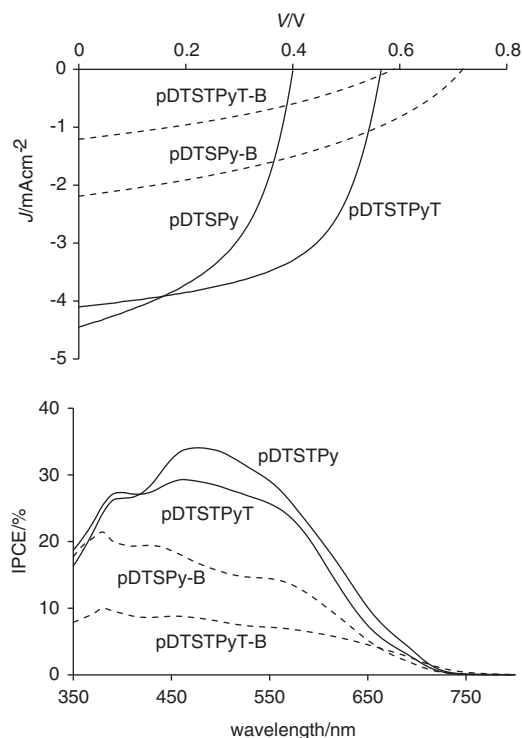


**Figure 3** *J*-*V* profiles (top) and IPCE spectra (bottom) of BHJ-type PSCs based on the DTS-pyridine polymers and their complexes.

bands with highly red-shifted absorption edges. The ionization potentials that corresponded approximately to the HOMO (highest occupied molecular orbital) levels were measured in air for films of **pDTSPy** and **pDTSPy-B** via photoelectron yield spectroscopy to be  $-5.23$  and  $-5.44$  eV, respectively, which again indicates that complex formation decreased the HOMO levels. The LUMO (lowest unoccupied molecular orbital) energy levels of these films were then calculated to be  $-3.26$  and  $-3.79$  eV based on the ionization potentials and the optical band gaps of these films. These results are in good agreement with the electronic states of PEDOT:PSS (HOMO:  $-5.0$  eV) and PC<sub>71</sub>BM (HOMO:  $-6.0$  eV, LUMO:  $-4.3$  eV).

### Applications to OPV

To explore the utility of the polymers used in this study and their complexes as host materials for BHJ-type PSCs, cells were fabricated based on blend films of the polymers and PC<sub>71</sub>BM (ITO/PEDOT:PSS/polymer:PC<sub>71</sub>BM (1:2.0 wt)/LiF/Al), with an active area of 0.25 cm<sup>2</sup>. The current density-voltage (*J*-*V*) curves and the incident photon-to-current conversion efficiency (IPCE) spectra of the cells are depicted in Figure 3, and the cell parameters are summarized in Table 2. The IPCE spectra are in agreement with the UV-Vis absorption spectra of

**Table 2** Photovoltaic properties of DTS-pyridine-based polymers

OPV	Polymer	$J_{sc}$ (mA cm <sup>-2</sup> )	$V_{oc}$ (V)	FF	PCE (%)
BHJ-PSC <sup>a</sup>	<b>pDTSTPyT</b>	4.07	0.56	0.58	1.33
	<b>pDTSPy</b>	4.28	0.39	0.55	0.83
	<b>pDTSTPyT-B</b>	1.21	0.59	0.35	0.25
	<b>pDTSPy-B</b>	2.21	0.71	0.39	0.61
DSSC <sup>b</sup>	<b>pDTSTPyT</b>	2.03	0.39	0.69	0.55
	<b>pDTSPy</b>	2.17	0.40	0.63	0.54

Abbreviations: BHJ, bulk heterojunction; DSSC, dye-sensitized solar cell; DTS, dithienosilole; FF, fill factor; OPV, organic photovoltaic cell; PCE, power-conversion efficiency; PSC, polymer solar cell.

<sup>a</sup>ITO/PEDOT:PSS/polymer:PC<sub>71</sub>BM (1:2.0 wt)/LiF/Al.

<sup>b</sup>FTO/polymer-attached TiO<sub>2</sub>/LiI<sub>2</sub> in acetonitrile/Pt.

the polymer blend films and the polymer complexes with PC<sub>71</sub>BM, although the IPCE edges of the cells with complex polymers were at approximately 750 nm, slightly shorter than the optical edges of the blend films (800 nm). The cell with **pDTSPy** exhibited a lower power-conversion efficiency (PCE) than the cell based on **pDTSTPyT** due to a lower open circuit voltage ( $V_{oc}$ ). Although the reason for the different  $V_{oc}$  between these cells is still unclear, the lower degree of incorporation of pyridine units in **pDTSPy** seems to affect the

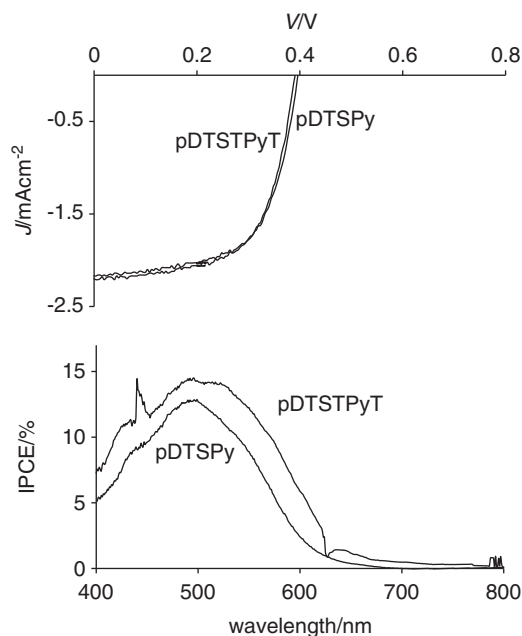


**Figure 4**  $J$ - $V$  profiles (top) and IPCE spectra (bottom) of DSSCs based on the DTS-pyridine polymers.

$V_{oc}$  to some extent. Interestingly, the use of complex polymeric pDTSTPyT-B and pDTSPy-B increased  $V_{oc}$ , although the close circuit current density ( $J_{sc}$ ) was largely suppressed to lower the PCE. In the present study, we found that annealing the active layers and the devices did not affect subsequent cell performance.

Pyridine-containing D-A-type compounds have been recently studied as sensitizing dyes for DSSC.<sup>25</sup> In this case, pyridine functions not only as an acceptor unit but also as an anchoring unit that can coordinate with Lewis acid sites of  $TiO_2$  to attach the dye to the  $TiO_2$  surface; this pyridine-Ti anchor is known to facilitate electron injection from the photo-excited dye, compared with the conventional ester anchor. Based on this property, we applied the pDTSTPyT and pDTSPy polymers to DSSC.  $TiO_2$  electrodes were immersed in solutions of polymer in chloroform at room temperature to give polymer-attached  $TiO_2$ ; DSSCs were fabricated with an FTO/polymer-attached  $TiO_2/LiI_2$  in acetonitrile/Pt structure. As shown in Table 2 and Figure 4, the DSSCs formed using these polymers exhibited a clear response, with PCEs of 0.55% and 0.54% for the cells containing pDTSTPyT and pDTSPy, respectively.

## CONCLUSION

In conclusion, we prepared new D-A-type polymers using dithienyl-DTS and DTS as the donors and using pyridine as the acceptor. Although these polymers exhibited limited  $\pi$ -conjugation, likely due to their twisted structures and to the rather weak D-A interaction, potential applications of these polymers to BHJ-type PSCs and DSSCs were also explored. Interestingly, complex formation upon  $B(C_6F_5)_3$  coordination enhanced the D-A interaction of the polymers. Furthermore, complex formation led to a higher  $V_{oc}$  of the BHJ-type PSCs compared with that of either pDTSTPyT- or pDTSPy-based PSCs. The present cells with complex polymers exhibited relatively low PCE, which was ascribed to the low  $J_{sc}$ , because the maximal PCE based on DTS-polymers was reported to be 7.3% for a DTS-thienopyrrolodione alternate polymer.<sup>14</sup> The increase in  $V_{oc}$  caused by complex formation provides useful information for the molecular design of efficient PSC materials.

## ACKNOWLEDGEMENTS

This work was supported by a Grant-in-Aid for Scientific Research on Innovative Areas, 'New Polymeric Materials Based on Element-Blocks (No.2401)' (24102005), from the Ministry of Education, Culture, Sports, Science, and Technology, Japan.

- Brabec, C. J., Gowrisanker, S., Halls, J. J. M., Laird, D., Jia, S. & Williams, S. P. Polymer-fullerene bulk-heterojunction solar cells. *Adv. Mater.* **22**, 3839 (2012).
- Chen, J. & Cao, Y. Development of novel conjugated donor polymers for high-efficiency bulk-heterojunction photovoltaic devices. *Acc. Chem. Res.* **42**, 1709 (2009).
- Ooyama, Y. & Harima, Y. Molecular designs and syntheses of organic dyes for dye-sensitized solar cells. *Eur. J. Org. Chem.* 2903 (2009).
- Chen, J. & Cao, Y. Silole-containing polymers: chemistry and optoelectronic properties. *Macromol. Rapid Commun.* **28**, 1714 (2007).
- Ohshita, J. Conjugated oligomers and polymers containing dithienosilole units. *Macromol. Chem. Phys.* **210**, 1360 (2009).
- Ohshita, J., Kai, H., Takata, A., Iida, T., Kunai, A., Ohta, N., Komaguchi, K., Shiotani, M., Adachi, A., Sakamaki, K. & Okita, K. Effects of conjugated substituents on the optical, electrochemical, and electron-transporting properties of dithienosiloles. *Organometallics* **20**, 4800 (2001).
- Kim, D.-H., Ohshita, J., Lee, K.-H., Kunugi, Y. & Kunai, A. Synthesis of  $\pi$ -conjugated oligomers containing dithienosilole units. *Organometallics* **25**, 1511 (2006).
- Zeng, W., Cao, Y., Bai, Y., Wang, Y., Shi, Y., Zhang, M., Wang, F., Pan, C. & Wang, C. Efficient dye-sensitized solar cells with an organic photosensitizer featuring orderly conjugated ethylenedioxythiophene and dithienosilole blocks. *Chem. Mater.* **22**, 1915 (2010).
- Ohshita, J., Nodono, M., Kai, H., Watanabe, T., Kunai, A., Komaguchi, K., Shiotani, A., Okita, K., Harima, Y., Yamashita, K. & Ishikawa, M. Synthesis and optical, electrochemical, and electron-transporting properties of silicon-bridged bithiophenes. *Organometallics* **18**, 1453 (1999).
- Hou, J., Chen, H.-Y., Zhang, S., Li, G. & Yang, Y. Synthesis, characterization, and photovoltaic properties of a low band gap polymer based on silole-containing polythiophenes and 2,1,3-benzothiadiazole. *J. Am. Chem. Soc.* **130**, 16144 (2008).
- Peet, J., Wen, L., Byrne, P., Rodman, S., Forberich, K., Shao, Y., Drolet, N. & Gaudiana, R. Bulk heterojunction solar cells with thick active layers and high fill factors enabled by a bithiophene-co-thiazolothiazole push-pull copolymer. *Appl. Phys. Lett.* **98**, 043301 (2011).
- Subramanian, S., Xin, H., Kim, F. S., Shoaee, S., Durrant, J. R. & Jenekhe, S. A. Effects of side chains on thiazolothiazole-based copolymer semiconductors for high performance solar cells. *Adv. Energy Mater.* **1**, 854 (2011).
- Subramanian, S., Xin, H., Kim, F. S. & Jenekhe, S. A. New thiazolothiazole copolymer semiconductors for highly efficient solar cells. *Macromolecules* **44**, 6245 (2011).
- Chu, T.-Y., Lu, J., Beaupre, S., Zhang, Y., Pouliot, J.-R., Wakim, S., Zhou, J., Leclerc, M., Li, Z., Ding, J. & Tao, Y. Bulk heterojunction solar cells using thieno[3,4-c]pyrrole-4,6-dione and dithieno[3,2-b:2',3'-d]silole copolymer with a power conversion efficiency of 7.3%. *J. Am. Chem. Soc.* **133**, 4250 (2011).
- Welch, G. C., Coffin, R., Peet, J. & Bazan, G. C. Band gap control in conjugated oligomers via Lewis acids. *J. Am. Chem. Soc.* **131**, 10802 (2009).
- Welch, G. C. & Bazan, G. C. Lewis acid adducts of narrow band gap conjugated polymers. *J. Am. Chem. Soc.* **133**, 4632 (2011).
- Hayashi, S., Asano, A. & Koizumi, T. Modification of pyridine-based conjugated polymer films via Lewis acid: halochromism, characterization and macroscopic gradation patterning. *Polym. Chem.* **2**, 2764 (2011).
- Hayashi, S. & Koizumi, T. Two synthetic approaches from 2,5-di(2-thienyl)pyridine to a  $BF_3$ -modified polymer film. *Chem. Lett.* **41**, 979 (2012).
- Khan, M. S., Al-Mandhary, M. R. A., Al-Suti, M. K., Feeder, N., Nahar, S., Köhler, A., Friend, R. H., Wilson, P. J. & Raithby, P. R. Synthesis, characterisation, and electronic properties of a series of platinum(II) poly-ynes containing novel thienyl-pyridine linker groups. *J. Chem. Soc. Dalton Trans.* 2441 (2002).
- Ohshita, J., Miyazaki, M., Zhang, F.-B., Tanaka, D. & Morihara, M. Synthesis and properties of dithienometalole-pyridinochalcogenadiazole alternate polymers. *Polymer J* **45**, 979-984 (2013).
- Ohshita, J., Kangai, S., Yoshida, H., Kunai, A., Kajiwara, S., Ooyama, Y. & Harima, Y. Synthesis of organosilicon polymers containing donor-acceptor type  $\pi$ -conjugated units and their applications to dye-sensitized solar cells. *J. Organomet. Chem.* **692**, 801 (2007).
- Ohshita, J., Kimura, K., Lee, K.-H., Kunai, A., Kwak, Y.-W., Son, E.-C. & Kunugi, Y. Synthesis of silicon-bridged polythiophene derivatives and their applications to el device materials. *J. Polym. Sci. Part A, Polym. Chem.* **45**, 4588 (2007).
- Lu, G., Usta, H., Risko, C., Wang, L., Facchetti, A., Ratner, M. A. & Marks, T. J. Synthesis, characterization, and transistor response of semiconducting silole polymers with substantial hole mobility and air stability. Experiment and theory. *J. Am. Chem. Soc.* **130**, 7670 (2008).
- Farfán, N. & Contreras, R. Carbon-13 nuclear magnetic resonance spectroscopy as a method to determine relative acidity of boron Lewis acids in pyridine complexes. *J. Chem. Soc. Perkin Trans. II* **771**, (1987).
- Ooyama, Y., Nagano, T., Inoue, S., Imae, I., Komaguchi, K., Ohshita, J. & Harima, Y. Dye-sensitized solar cells based on donor- $\pi$ -acceptor fluorescent dyes with a pyridine ring as an electron-withdrawing-injecting anchoring group. *Chem. Eur. J.* **17**, 14837 (2011).